scientific reports

Check for updates

OPEN

Sustained alterations in proximal tubule gene expression in primary culture associate with HNF4A loss

Asha C. Telang, Jenna T. Ference-Salo, Madison C. McElliott, Mahboob Chowdhury & Jeffrey A. Beamish✉

Primary cultures of proximal tubule cells are widely used to model the behavior of kidney epithelial cells in vitro. However, de-differentiation of primary cells upon culture has been observed and appreciated for decades, yet the mechanisms driving this phenomenon remain poorly understood. This confounds the interpretation of experiments using primary kidney epithelial cells and prevents their use to engineer functional kidney tissue ex vivo. In this report, we measure the dynamics of cell-state transformations in early primary culture of mouse proximal tubules to identify key pathways and processes that correlate with and may drive de-differentiation. Our data show that the loss of proximal-tubule-specific genes is rapid, uniform, and sustained even after confluent, polarized epithelial monolayers develop. This de-differentiation occurs uniformly across many common culture condition variations. Changes in early culture were strongly associated with the loss of HNF4A. Exogenous re-expression of HNF4A can promote expression of a subset of proximal tubule genes in a de-differentiated proximal tubule cell line. Using genetically labeled proximal tubule cells, we show that selective pressures very early in culture influence which cells grow to confluence. Together, these data indicate that the loss of in vivo function in proximal tubule cultures occurs very early and suggest that the sustained loss of HNF4A is a key regulatory event mediating this change.

In the United States alone, over 800,000 patients suffer from end-stage kidney disease (ESKD). Despite decades of research[1,2], few new therapies for ESKD have emerged. Though kidney epithelial cells can regenerate, bioengineered alternatives to dialysis that harness this potential remain elusive. In part, this shortcoming is due to an inability to recapitulate the physiology of proximal tubule cells ex vivo.

Cell culture is widely used to model the behavior of cells and tissues in vitro. Many regenerative and modeling approaches also rely on cultured cells[3–7]. Cell culture facilitates experimental manipulations and generates samples amenable to most analytical and molecular techniques that may be difficult to apply in vivo. However, to achieve these advantages, routine culture is optimized for cell growth and convenience. The resulting conditions often differ dramatically from those in vivo, including supraphysiologic growth factor concentrations, diffusion-limited nutrient transport, and ultra-rigid plastic tissue culture substrates.

Generally, primary cultured cells are labeled according to their tissue of origin. This approach assumes cultured cells retain gene expression patterns and pathways that govern in vivo function. However, for highly specialized cells, such as epithelial cells in the kidney proximal tubule, many pathways[8–11]and morphologic characteristics[12–15]are lost early in culture. Kidney organoid models can generate proximal tubules with many in vivo characteristics[16,17]. However, these models are less amenable to high-throughput analyses possible with standard cell culture systems accessible to most researchers. We now know that cell lines used widely to model proximal tubule function lack expression of most metabolic and transport genes indicative of proximal tubule epithelial cells in vivo[18]. These findings indicate that the physiological state of proximal tubule cells is unstable in culture. The rapid morphological and biochemical alterations observed in early primary proximal tubule cultures suggest that this instability manifests early. A lack of a detailed molecular understanding of how and why such transformations occur limits the utility of proximal tubule cultures to model disease or restore kidney function ex vivo.

Though cell changes in proximal tubule cultures have been studied extensively over the last 4 decades[4,7,9,10,12,19–22], most studies predate the advent of accessible high-throughput sequencing techniques to assess genome-wide expression changes. Our goal was to measure the dynamics of cell-state transformations in early primary culture to identify key pathways and processes that result in de-differentiated cell populations in culture. Surprisingly, we found that the loss of proximal-tubule-specific genes occurs rapidly and permanently.

Division of Nephrology, Department of Internal Medicine, University of Michigan, 1500 E. Medical Center Drive, SPC 5364, Ann Arbor, MI 48109, USA. ✉email: jebeamis@med.umich.edu

No evidence of re-expression of most genes was seen even after confluent, polarized epithelial monolayers develop. These changes were strongly associated with loss of the transcription factor Hepatocyte Nuclear Factor 4 alpha (HNF4A). Using lineage-traced proximal tubule cells, we show that selective pressures early in culture influence which cells grow to confluence. Together, these data indicate that the loss of in vivo function occurs very early in culture and suggest the loss of HNF4A as a regulatory event mediating this change.

Results

Proximal tubules develop confluent, polarized epithelium in culture

Many isolation protocols exist for obtaining proximal-tubule-enriched samples[14,23]. We obtained a purified preparation of proximal tubules using enrichment by density gradient centrifugation. This method has been well established to preserve viability and metabolism during the isolation process[24,25] (Fig. 1a). The enriched preparations contained 84.2 ± 2.5% proximal tubules, marked with lotus lectin, which was enriched from 65.7 ± 5.8% (Supplementary Fig. S1) in unpurified aggregates of digested kidneys. Culture medium (see Methods) was adapted from established protocols[9,14,26]. Tubule retention after 1 day was low (Fig. 1b). Many of the unattached tubules displayed granular morphology consistent with synchronized tubule death reported by others[27]. Surviving cells formed colonies with epithelial morphology that grew to confluence by 7–10 days of

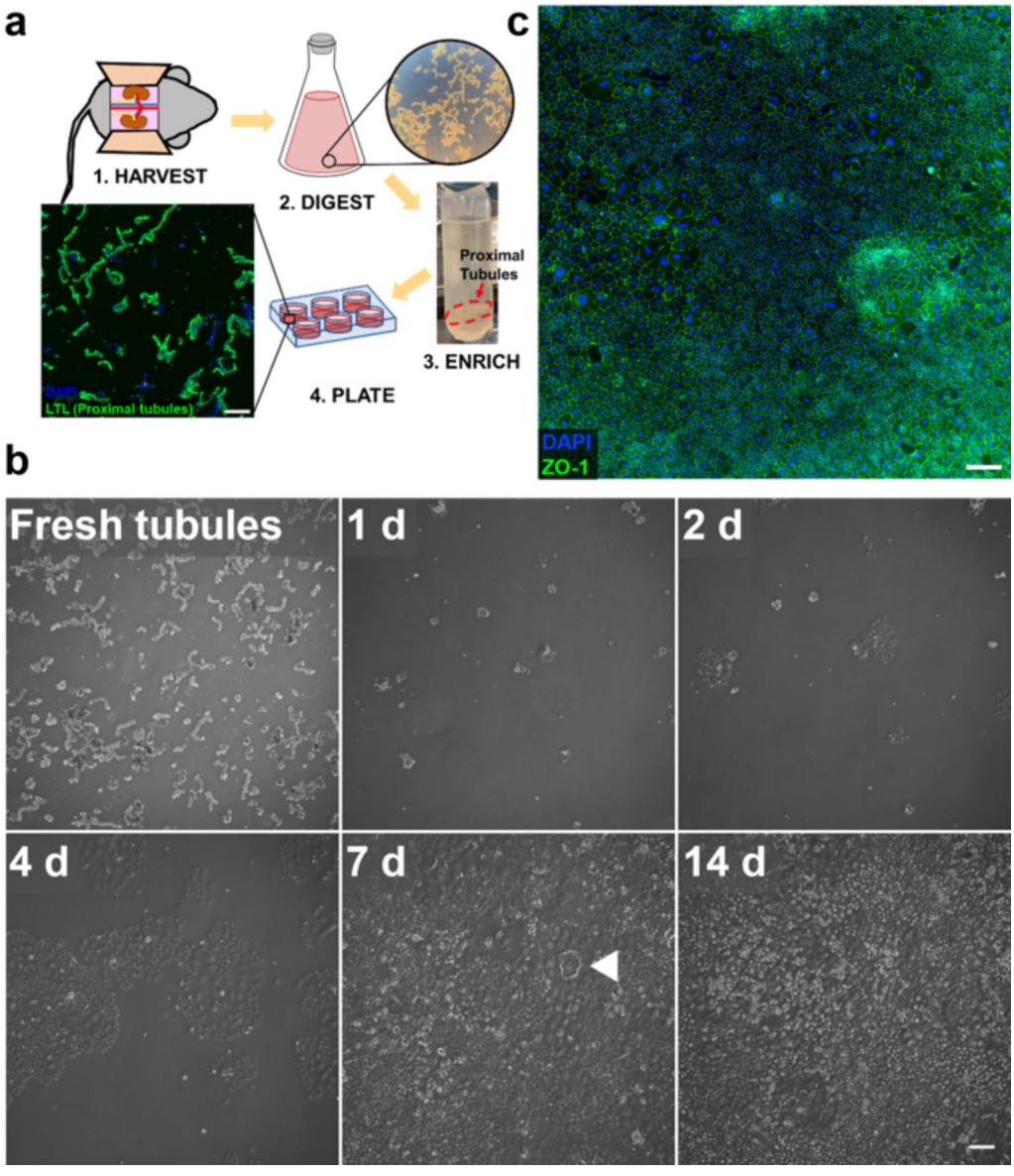

Fig. 1. Proximal tubules develop polarized epithelium in culture. (**a**) Proximal tubules were isolated and enriched from minced kidneys using collagenase digestion followed by gradient centrifugation and cultured for 14 days (see "Methods", scale bar 200 µm). (**b**) Phase contrast micrographs of typical cultures over 14 days (scale bar 100 µm). Arrowhead indicates an example of dome formation. (**c**) Staining for zonula occludens-1 (ZO-1) shows development of epithelial morphology throughout the culture (scale bar 200 µm).

culture (Fig. 1b). The resulting cultures showed uniform zonula occludens-1 (ZO-1) expression (Fig. 1c) and, in some areas, formed polarized cuboidal (approximately 10×10×10 µm) epithelium with apical ZO-1 and basolateral sodium potassium ATPase (Supplementary Fig. S2). This also indicates low levels of non-epithelial contaminant cell populations, such as fibroblasts. Dome formation[8,14], which reflects the formation of tight junctions with transepithelial transport, was occasionally observed at the onset of confluence (day 7) but was lost with ongoing culture (Fig. 1b). These data establish that our methodology yields a tubule-derived epithelial monolayer consistent with the results reported by others.

Proximal-tubule-specific gene expression is rapidly and irreversibly lost in culture

Primary culture of proximal tubules may preserve expression of some genes specific to the proximal tubule[18]. To investigate this in detail, we measured the expression profile of proximal tubule cells during primary culture using bulk RNA sequencing (Fig. 2a). In our initial analysis, we focused on a curated list of 193 proximal-tubule-specific genes derived from microdissected rat tubules[28]and previously used as a measure of similarity to native proximal tubule cells[18]. This gene set is comprised of genes expressed in each of the three proximal tubule segments, S1, S2, and S3, in roughly equal proportions. The proximal tubule preparations were highly enriched in the expression of the proximal-tubule-specific genes (Fig. 2b, Day 0) with 78% (149 of 193) with a TPM > 15, a fraction consistent with that previously reported for microdissected mouse proximal tubule[18,29]. Surprisingly, we found a near-uniform, rapid, and sustained loss of this gene set within the first 2 days of culture (Fig. 2b, Supplementary Data S1, Supplementary Data S2). Even as cells developed confluent, polarized epithelial monolayers by 7–14 days (Fig. 1b), there was no evidence of re-expression of most proximal tubule genes. Gene Set Enrichment Analysis (GSEA) revealed that proximal-tubule-selective genes were strongly enriched among the downregulated genes as early as 1 day after plating ($P_{adj} = 1 \times 10^{-32}$) and remained so throughout the culture experiment (14 days, $P_{adj} = 6 \times 10^{-50}$, Fig. 2c). Likewise, when proximal tubule segment-specific gene sets, identified by unbiased clustering of single nucleus RNA sequencing data by Kirita et al.[30] were substituted, all segments showed robust downregulation within 1 day of culture that persisted (Supplementary Fig. S3). Taken together, these data suggest that the expression of most genes that define the specific functions of the proximal tubule are lost almost immediately in culture.

Transition to culture is characterized by activation of stress and inflammatory pathways

To better define the pathways associated with dedifferentiation, we performed GSEA against the Molecular Signatures Database Hallmark Genesets[31]. Many processes associated with the mature proximal tubule were lost early in culture including oxidative metabolism, fatty acid metabolism, and xenobiotic metabolism (which includes many transporters) (Fig. 3a). In contrast, three groups of Gene-set-associated processes were upregulated. Early culture samples were highly enriched with stress response genes including TNFα signaling via NFκB. Transcript levels of *Tnf*(TNFα) and two downstream targets associated with progression of kidney disease[32], *Ccl2* and *Timp1*, increased significantly at 1 d and were sustained (Fig. 3b, Supplementary Fig. S4). Mid-culture samples (2–7 days) were enriched with pathways associated with mitosis consistent with increased *Mki67* expression (Supplementary Fig S4). Late culture was associated with the epithelial-to-mesenchymal transition gene set.

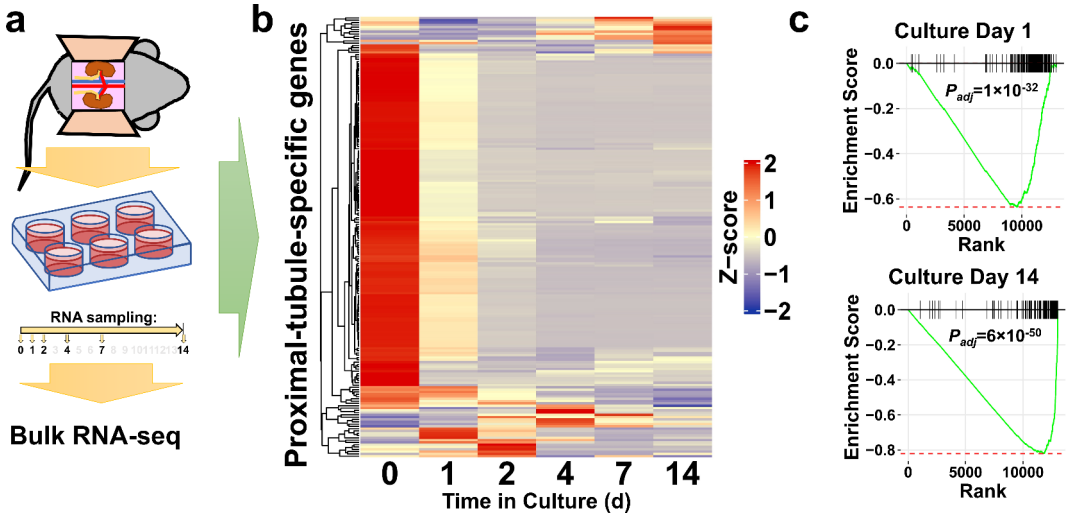

Fig. 2. Proximal-specific gene expression is rapidly and irreversibly lost in culture. (**a**) Overview of experimental timeline. (**b**) Heatmap of 193 proximal tubule genes used by Khundmiri, et al.[18] at selected times in primary culture. Day 0 reflects proximal tubules prior to plating but after enrichment. Row Z-scores are shown and are available in Supplementary Data S2. (**c**) Gene Set Enrichment Analysis (GSEA) plots for the proximal-tubule-specific gene set defined by Khundmiri, et al. in the differentially expressed genes from 1 d (vs. 0 day) and 14 days (vs. 0 day) of culture.

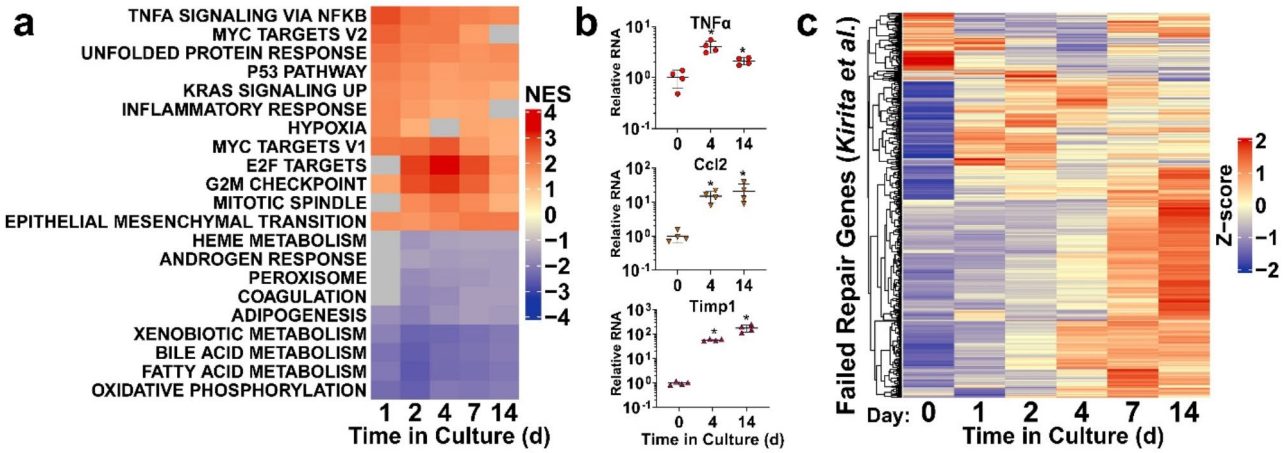

Fig. 3. Transition to culture is characterized by activation of stress and inflammatory pathways. (**a**) Gene Set Enrichment Analysis (GSEA) for all Molecular Signatures Database Hallmark Genesets[31] in the differentially expressed genes at the indicated timepoint relative to 0 d tubules. The normalized enrichment score (NES) is plotted as a heatmap. Only scores with an adjusted $P_{adj} < 0.05$ are colored (non-significant analyses are gray). Only gene sets with significant enrichment at 4 or 5 time points are shown for clarity (data for all pathways is available in Supplementary Data S2). (**b**) Expression of *Tnf* (TNFα), *Ccl2*, and *Timp1* from biologically independent samples using quantitative RT-PCR (corresponding RNA-seq data is shown in Supplementary Fig. S4, $^*P \leq 0.015$, ANOVA with Tukey post hoc test, $N = 4$) (**c**) Z-score normalized heatmap of the marker genes that defined the failed repair cluster identified by Kirita et al.[30].

This pattern of inflammatory and stress signatures, followed by proliferation, leading to loss of epithelial differentiation is similar to the path followed by proximal tubules that fail to repair after ischemic injury identified in several recent single-cell studies[30,33–35]. Indeed, there was a rapid and sustained induction of *Havcr1* (also known as Kidney Injury Molecule 1, KIM-1). This pattern mirrors "failed repair" proximal tubules in vivo in which *Havcr1*is induced early after injury and is sustained even after recovery of nearby tubules[30] (Supplementary Fig. S4). When we mapped proximal tubule marker genes defined by Kirita et al.[30] to the cell culture data using GSEA[36–38], we found early enrichment of injury-associated genes and late enrichment of genes associated with "failed repair" proximal tubule cells (Supplementary Fig. S5, Supplementary Data S2). Primary cultures upregulated most of the "failed repair" genes, but only after cells reached confluence later in culture (Fig. 3c, Supplementary Data S2). Based on these findings, we hypothesized that inhibiting this inflammatory activation via TNFα or NFκB may delay de-differentiation. However, in the presence of inhibition of TNFα or NFκB, tubules failed to attach and grow (Supplementary Fig. S6), suggesting that activation of these pathways is essential to establish cultured cells.

De-differentiation in culture is tightly associated with loss of HNF4A activity

To define the key transcriptional pathways driving dedifferentiation in culture, we submitted the differentially expressed genes at 1 day of culture to ChEA3[39], which compares this list with multiple libraries of chromatin immunoprecipitation sequencing (ChIP-seq) data to infer transcription factor targets. Transcription factors associated with early upregulated genes included FOSL1, MYC, and ATF3, which was consistent with the GSEA analysis above that highlighted stress-response pathways (Supplementary Data S3). For downregulated genes, HNF4A was the most highly associated transcription target and was central to a network of associated transcription factors including HNF4G and NR1H4 (also known as Farnesoid X receptor, Fig. 4a, Supplementary Data S3). Both HNF4A[30,34]and NR1H4[40]play a critical role in acute kidney injury while HNF4G is likely a redundant transcription factor in the proximal tubule[41]. Moreover, HNF4A is critical for the development of the mature proximal tubule[42].

Recently, Marable et al. used a combination of ChIP-seq and RNA-seq in early kidney development to identify genes likely regulated by HNF4A in the proximal tubule[42]. A heatmap of these HNF4A targets shows rapid loss of proximal-tubule-specific HNF4A target expression, including *Pck1* and *Slc34a1* (Fig. 4b-c, Supplementary Data S1). Though similar in appearance to Fig. 2b, only 56 of the 193 proximal tubule genes[18] (29%) were also HNF4A targets. Those genes that overlap were uniform in their loss of expression with culture. Expression of *Hnf4a* drops by several orders of magnitude in just the first few days of culture (Fig. 4c, Supplementary Fig. S7). Differentially downregulated genes were highly enriched with HNF4A targets early in culture and after reaching confluence, highlighting that re-expression of this pathway does not occur (Fig. 4d). These data suggest that HNF4A and its targets are silenced early in primary culture.

If HNF4A loss results in the loss of PT-specific genes in primary cultures, we hypothesized that re-expression of HNF4A could restore some proximal tubule gene expression, as has been shown in trans-differentiation studies with fibroblasts[43]. Silencing of HNF4A expression is also common in most stable proximal tubule cell lines[18]. Our initial studies indicated a low transduction efficiency using an established HNF4A over-expressing retroviral vector[44]. Rather than transducing primary cultures, we used the BUMPT proximal tubule cell line[45–47]

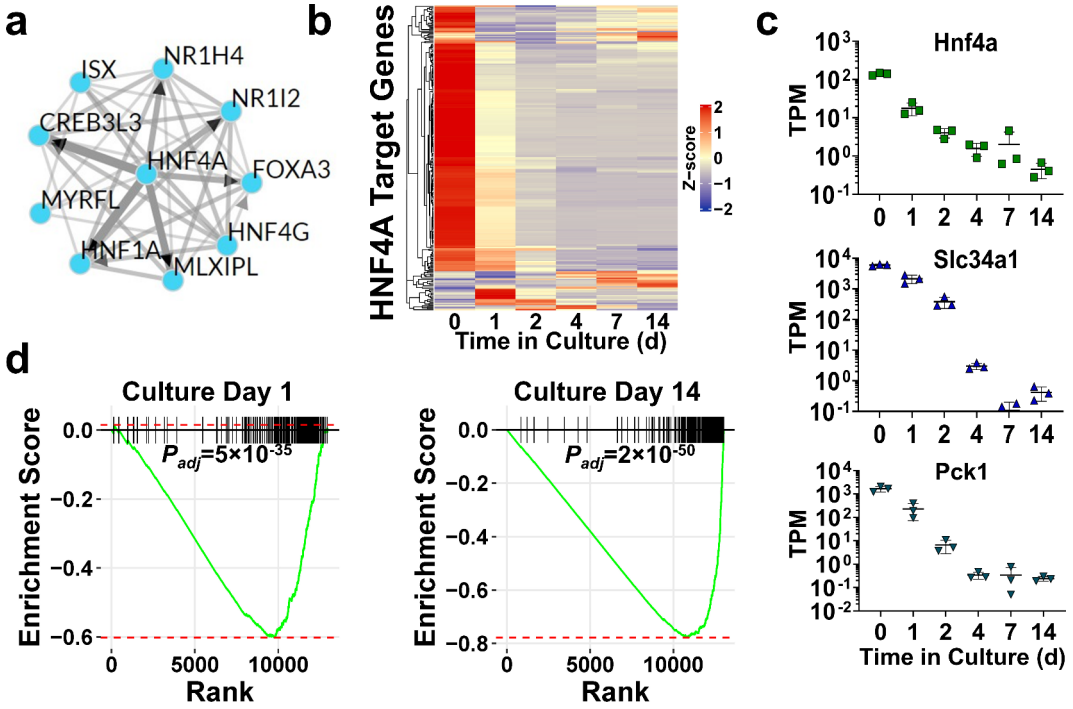

Fig. 4. HNF4A activity is central to expression changes in culture. (**a**) ChEA3[39] transcription factor network map of genes downregulated in the first day after plating. Full results are available in Supplementary Data S3. (**b**) Heatmap of proximal tubule HNF4A targets[42] in cultured cells over time. Row Z-scores are shown and are available in Supplementary Data S2. (**c**) Expression of *Hnf4a* and two of its proximal tubule targets, *Slc34a1* and *Pck1*. Confirmatory quantitative RT-PCR from independent samples are shown in Supplementary Fig S7. (**d**) Gene Set Enrichment Analysis (GSEA) plots for HNF4A target genes defined by Marable et al.[42] in the differentially expressed genes after 1 day (vs. 0 day) and 14 days (vs. 0 day) of culture.

which expresses 14% of proximal tubule genes with TPM > 15 (Supplementary Data S4). We generated 3 independent clones with stable expression of HNF4A and 3 controls. The differentially upregulated genes in the HNF4A over-expressing clones were strongly enriched for both proximal-tubule-specific genes[18]and HNF4A targets[42] (Supplementary Fig. S8). However, the overall changes in expression were modest with an increase to 22% of proximal tubule genes with TPM > 15 (P= 0.046, χ^2 test). These data suggest that re-expression of HNF4A only partly restores a robust proximal tubule phenotype in culture.

De-differentiation is unaffected by culture medium constituents

The composition of culture medium optimized for proximal tubules varies widely. To address the possibility that de-differentiation noted above was driven by suboptimal culture conditions we screened several alternative culture parameters previously shown to affect primary culture behavior. These included medium constituents such as glucose concentration[9], insulin concentration[9,48], epidermal growth factor[49], retinoic acid[50], and serum[51]. Furthermore, cells cultured on a porous insert can facilitate transport[52]. None of these maneuvers averted the silencing of HNF4A nor the significant upregulation of Havcr1 (KIM-1) (Fig. 5). Only epidermal growth factor (EGF) withdrawal significantly increased HNF4A expression, though it remained several orders of magnitude below that of native tubules. This effect was consistent with the known effects of EGF on metabolism and proliferation[49,53]. We also noted that low insulin and serum free conditions slowed growth resulting in a lower extent of confluency at 14 days (Supplementary Fig. S9). However, both conditions showed the same pattern of gene expression as others studied. This observation suggests that the degree of confluence is not a major contributor to the observed trends. Combined, these observations suggest that medium composition has minimal influence on long-term cultured cell behavior relative to native expression patterns.

Selective pressure in early culture determines the confluent culture population

There are distinct expression and metabolic profiles in the S1, S2, and S3 segments of the proximal tubule[28,30,54,55]. Since immediate survival and attachment upon culture is poor (Fig. 1b), whether cells from different proximal tubule segments have an equal chance of survival is unclear. Thus, the bulk transcriptome in culture could be impacted by preferential selection of specific proximal tubule subtypes or even from contaminating non-proximal tubule cells.

To assess this possibility, we genetically tagged mouse proximal tubules in vivo, prior to culture. Our strategy used mice with a phosphoenolpyruvate carboxykinase (PEPCK)-Cre driver with proximal-tubule-selective Cre expression (Supplementary Fig. S10)[38,56]. Mice also carried a reporter construct that expresses tdTomato in the absence of Cre recombinase. In the presence of Cre recombinase, the tdTomato gene is excised, enabling

a

Condition	Change
STD	Standard medium (Table 1)
TW STD	Transwell insert, standard medium
L GLU	Reduced glucose (85 mg/dL)
TW L GLU	Transwell insert, reduced glucose
L INS	Reduced insulin (20 ng/mL)
NO SERUM	No serum
NO SERUM D10	Serum withdrawn at 10 d
NO EGF D10	EGF withdrawn at 10 d
STD RA D12	Retinoic acid (100 nM) added at 12 d
NO SERUM RA D12	Serum withdrawn (10 d), Retinoic acid added (12 d)

b

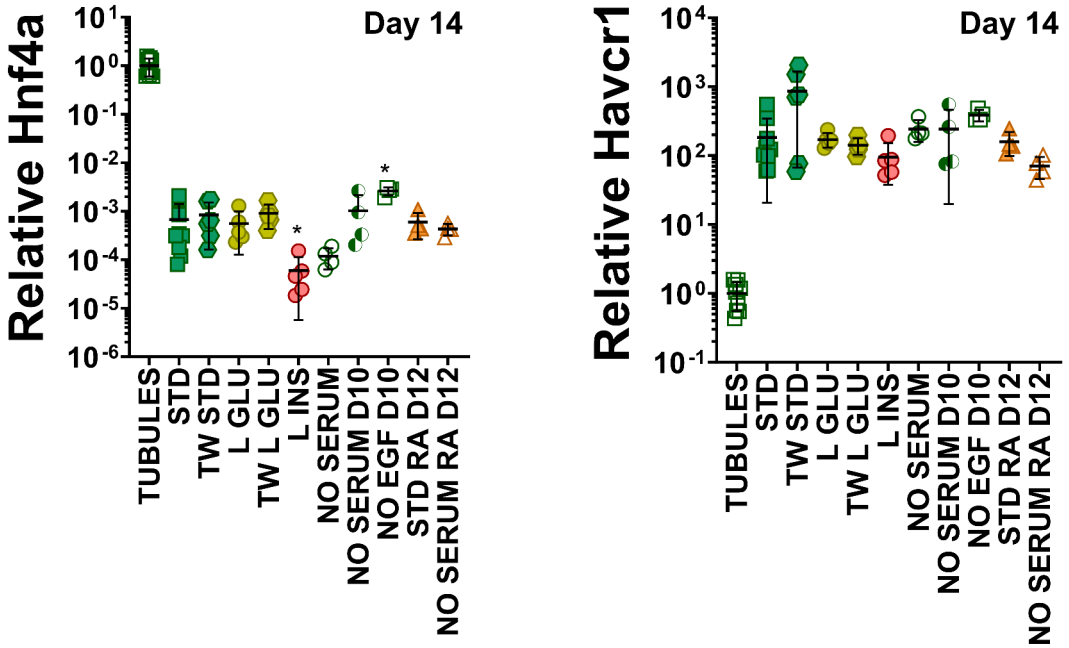

Fig. 5. De-differentiation is insensitive to culture conditions. (**a**) Legend and details for specific culture condition changes. (**b**) Quantitative RT-PCR for *Hnf4a* and *Havcr1* in fresh enriched proximal tubules (TUBULES) vs. 14 days cultures (*$P \leq 0.05$, ANOVA with Tukey post hoc test relative to standard conditions (STD) at 14 days; all samples were highly significant compared with tubules, $N = 4–9$).

the permanent expression of green fluorescent protein (GFP) (Supplementary Fig. S10). Two variations of the construct were used that express fluorescent reporters either in the cell membrane (mT/mG) or in the nuclear envelope (nT/nG). We previously showed that PEPCK-Cre, mT/mG mice label most S3 proximal tubule cells with less labeling of the S1 and S2 segments and with minimal labeling of non-proximal tubule segments[38] (Fig. 6a, Supplementary Fig. S10). PEPCK-Cre, nT/nG mice also show this pattern but with lower overall labeling efficiency compared with mT/mG. (Fig. 6a, Supplementary Fig. S11). In both strains, new labeling is unlikely in culture because there is rapid down-regulation of *Pck1* (Fig. 4c, Supplementary Fig. S7) whose promotor is homologous to the PEPCK-Cre construct[56]. Therefore, cell labeling using the PEPCK-Cre driver is locked in at the beginning of culture and can be used as a reliable indicator of cell lineage. Unlabeled cells still express the tdTomato fluorescent marker in the absence of Cre.

Upon primary culture, the fraction of GFP-positive cells was stable at day 1, but we observed a substantial loss of GFP-positive cells beyond 2 days (Fig. 6b,c). These data indicate that PEPCK-expressing proximal tubule cells are significantly depleted from culture. A second possibility is that sub-populations proliferate at different rates. At times beyond 4 days, many areas of the culture were near confluence, causing cell size to vary considerably. Therefore, the membrane-labeled cells could not be used to assess differences in proliferative capacity. To address this, we performed similar experiments using a nuclear-localized reporter (nT/nG). After epithelial islands were established, exponential growth from 2 to 7 days was identical between the two populations (Fig. 6d,f). This indicates that the primary driver of selection is survival during the initial few days of culture.

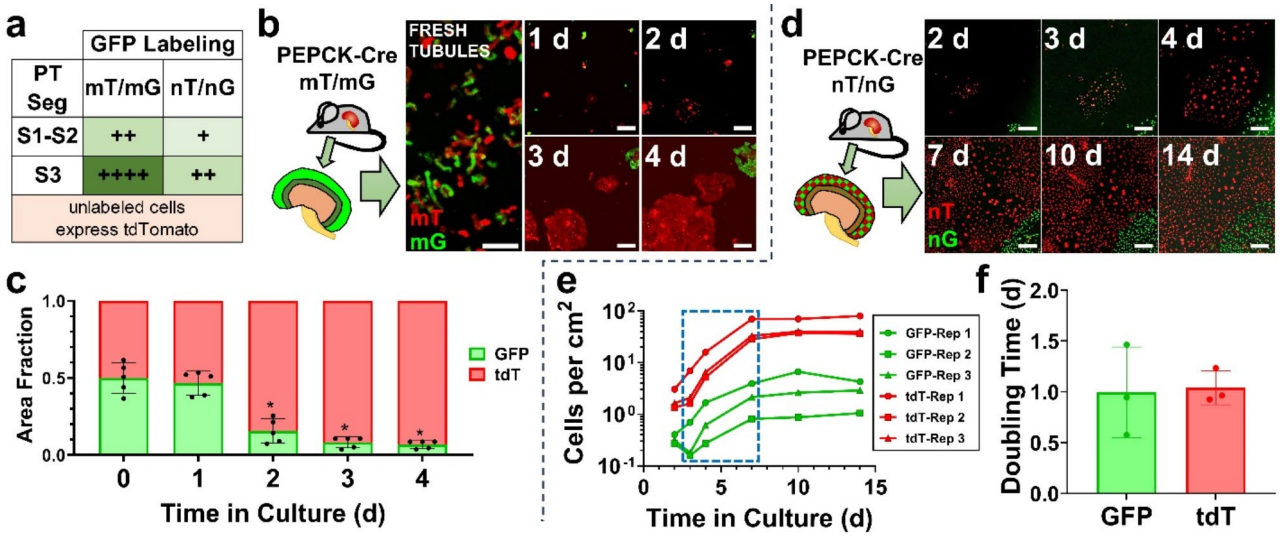

Fig. 6. Early culture selects against PEPCK expressing proximal tubules. (**a**) Summary of in vivo GFP labelling efficiency by proximal tubule segment (PT Seg) for each mouse strain used in the labeling studies. Additional data is shown in Supplementary Figs. S10 and S11. All unlabeled cells express tdTomato. (**b**) Tubules from 6-week-old female mice with a PEPCK-Cre driver and a membrane-bound tdTomato/GFP reporter (mT/mG) were cultured as in Fig. 1 and followed in early culture (0–4 days). Proximal tubule cells that expressed the PEPCK-Cre driver in vivo are stably marked by GFP. All other cells label with tdTomato (tdT) (**c**) The relative fraction of tdTomato vs. GFP area was used as a surrogate for cell population in early culture ($^*P < 0.05$, ANOVA with Tukey post hoc test relative to just after plating, 0 day, $N = 5$ independent experiments). (**d**) During growth, cell area varied and was a poor surrogate for cell proliferation. Therefore, the mT/mG reporter was replaced with a nuclear membrane localized tdTomato/GFP reporter (nT/nG). Tubules from these mice were cultured for 14 days. (**e**) After 2 days, individual nuclei were identifiable and used to quantify the populations of cells of each type. The average cell density for each independent replicate experiment ($N = 3$) is shown. (**f**) The doubling time was calculated during exponential growth (3–7 days, box) and was equivalent between GFP and tdTomato marked cells ($P = 0.88$, paired t-test). Scale bars 200 µm.

These studies could not distinguish between survival of unlabeled S1/2 cells or the small fraction of contaminating non-proximal tubule epithelial cells. To try to distinguish these possibilities, we examined enrichment of marker gene sets expressed in other nephron cell types[30]. Though we detected marker gene expression from contaminating tubular cell types in the tubule preparations, markers from nearly all nephron cell types were lost immediately in culture (Supplementary Fig. S12). Therefore, selective pressure alone does not explain the expression changes observed.

Discussion

Primary cultures of proximal tubules are widely used as models for proximal tubule physiology that may overcome many of the limitations of immortalized cell lines[18]. Our goal was to characterize the changes as native proximal tubules enter cell culture at a genome-wide scale. Our experiments revealed three key findings. First, primary proximal tubule cultures, though they may have epithelial morphology, lack expression of most proximal-tubule-specific genes when compared with their in vivo counterparts. Second, this transformation occurs almost immediately at the initiation of culture, is not reversed as cells become confluent, and is strongly associated with loss of HNF4A and its targets. Third, early loss of proximal tubule-specific gene expression is concurrent with a strong selective pressure that depletes cells derived from the S3 proximal tubule.

The loss of proximal tubule functions in cell culture has been observed for decades. However, primary proximal tubule cultures are widely used with the implicit assumption that primary proximal tubule cultures model in vivo cell behavior[23,47,57,58]. One goal of this work was to clarify the strengths and limitations of this model and to identify possible mechanisms driving the observed changes. The causes of proximal tubule de-differentiation were the topic of substantial study in the 1980s and 1990s[8–11,21,22,48,59]. These studies used tools available at that time including measurement of metabolites, cell death, and morphology. In aggregate, these studies demonstrated that proximal tubule functions in early culture are substrate-limited. If provided oxygen, which is diffusion-limited in static culture[60–62], and metabolic substrates in the form of fatty acids or lactate, then proximal tubule cultures can continue to perform functions such as gluconeogenesis for a time. Growth factors, such as insulin and EGF, also influence the rate of de-differentiation[9,48,49]. However, even under optimized conditions, cells invariably lose many specific proximal tubule functions in prolonged culture. This indicates that neither substrate availability nor changes in growth factor availability are the sole drivers of de-differentiation.

Consistent with these observations, a central finding of our work is that changes in proximal-tubule-specific gene expression are rapid, quantitatively large, and irreversible under standard conditions. Gene expression changes in early culture closely model that of ischemic injury and progression to a chronic "failed repair" state

rather than repair. These findings explain why proximal tubule substrate responses are strongest in the early culture period when the protein products of these genes are still present. The fact that prolonged culture parallels "failed repair" is consistent with metabolic changes associated with chronic injury[63]. Furthermore, we noted inflammatory pathways are correlated with de-differentiation. However, inhibition of these pathways blocks the establishment of cells in culture. This observation suggests that proliferation and differentiation are mutually exclusive. Similarly, proximal tubules provided with oxygen and fatty acid substrates showed more differentiated metabolism but slower growth[8,11,21]. In vivo, the established paradigm for repair requires de-differentiation before proliferation and is consistent with decades of studies on AKI[64]. These features highlight the potential utility of primary cultures to model AKI recovery but may limit their use for investigating normal proximal tubule physiology.

Our analysis identified the loss of HNF4A as a key event in de-differentiation. HNF4A is critical for the establishment of unique proximal tubule metabolism in kidney development[42]. In ischemic AKI, the re-expression of HNF4A tightly correlates with successful repair whereas failed repair cells do not express HNF4A[30,34]. However, the regulation of HNF4A expression in the normal and regenerating proximal tubule is not well defined. HNF4A is also expressed in the gastrointestinal tract, including the liver and pancreas, where it is regulated by oxygen tension, likely independently of hypoxia-inducible factor[65,66]. However, our finding that overexpression of HNF4A alone in the proximal tubule cell line BUMPT did not restore expression of many in vivo HNF4A targets suggests other factors are required or epigenetic changes have rendered HNF4A targets inaccessible. However, our findings suggest that primary cultures could be an excellent model for studying factors that control dynamic HNF4A expression and target accessibility during repair in vivo.

Many variables affect proximal tubules in culture. Exploring this parameter space exhaustively was beyond the scope of this study, nor was our goal to develop optimized culture conditions. Instead, we selected culture conditions that would be accessible to most labs and that reflect the way primary cultures are used in most studies, most commonly static culture on tissue culture plastic. However, other variables and conditions may be important, but are not widely implemented. Medium flow induced by oscillatory motion exerts shear stress on the cultured cells and facilitates transport of oxygen and other metabolites[8,10,20,67]. The elasticity[12,13,68]and composition[15]of the cell substrate influence gene expression, proliferation, and growth factor presentation. We also did not include TGF-B1 inhibition which helps to reinduce some proximal tubule markers and functions[12,69–71], though our data does indicate a substantial and sustained increase in expression of TGF-B1 that also parallels de-differentiation (Supplementary Data S1). Likewise, we did not test TNFα inhibition at later times after monolayers were established. Like inhibition of TGF-B1, TNFα inhibition at later times might support re-expression of some proximal tubule genes. Furthermore, proximal tubules in cultured kidney organoids can attain many features of mature proximal tubule in vivo[16,72]. However, proximal tubule cells isolated and cultured from organoids also de-differentiate[73]. These observations are consistent with our study and highlight the role of the 3D architecture and communication with surrounding interstitial cells present in organoid models but not in routine culture. Exploring these parameters with the approaches and tools outlined here is an important next step.

The strong selective pressure observed early in culture highlights the critical need for strategies that optimize conditions from the moment of isolation. This was well appreciated in the studies from the last century but, to our knowledge, has not been explored in detail recently. Our results highlight that proximal tubule cells that label with the PEPCK-Cre driver in vivo, which can mark differentiated proximal tubule in all segments but especially the S3 segment, are subject to negative selection. The low labeling efficiency of our model limited our ability to differentiate between non-PEPCK-expressing proximal tubule cells and other nephron segments. However, our transcriptomic analysis indicates that markers with segment specificity in vivo cannot be used reliably to infer cell lineage in culture since marker profiles for nearly all differentiated nephron segments (including those originating from contaminating non-proximal tubules) were downregulated.

Our studies provide important data about the dynamics of gene expression changes that explain the de-differentiation of proximal tubule cells in culture. We highlight key molecular events that underpin the limitations of cultured cells to recapitulate the functions of the kidney ex vivo. This data will provide important context for experiments obtained from primary culture models and will facilitate the next generation of approaches to model kidney diseases in vitro and to bioengineer alternatives to dialysis for patients suffering from kidney disease.

Methods

Animals

All studies involving mice were approved by the Institutional Animal Care and Use Committee at the University of Michigan and performed in accordance with the National Institutes of Health *Guide for the Care and Use of Laboratory Animals* and in accordance with ARRIVE guidelines. Wild type mice used in experiments were strain C57BL/6J purchased from Jackson Labs (stock number 000664). Two strains of proximal tubule tagged mice were used. Cre sensitive reporter strains expressing either plasma membrane (Gt[Rosa]26Sor$^{tm4[ACTB-tdTomato,-EGFP]luo}$, Jackson Labs, stock number 007676, mT/mG) or nuclear envelope (Gt(ROSA)26Sor$^{tm1(CAG-tdTomato*,-EGFP*)Ees}$, Jackson Labs, stock number 023537, nT/nG) fluorescence tags[74]were bred with mice containing a phosphoenolpyruvate carboxykinase (PEPCK) Cre driver, obtained from Volker H. Haase[56]. New strains were bred to homozygosity at all transgenic alleles.

Proximal tubule preparation

Unless specified, all reagents were purchased from Thermo-Fisher Scientific and were of cell culture grade or better. Procedures were adapted from those previously published[24,25]. Briefly, per experiment, 2–3 6-week-old female mice were euthanized by CO_2 overdose. Kidneys were immediately explanted and placed in ice-cold

MEM (Gibco, 11095080) buffer equilibrated with 95% O_2/5% CO_2(pH 7.4) and supplemented with 5 mM lactate (Sigma, L1750-10G), 5 mM glycine (Fisher, BP381-500) and 1 mM alanine (Sigma, 05129) (MEM + LGA). Kidneys were then decapsulated and minced into 1 mm^3 pieces by rapid chopping with a fresh razor blade on an ice-cold tile. Minced kidney was placed in ~ 1.4 mg/mL collagenase type 1 (Worthington, LS004196) in MEM + LGA supplemented with 2 mM heptanoic acid (Fisher, 164172500), 25 mM mannitol (Sigma, M9647), and 2.5 mg/mL albumin (Proliant Biologicals, 68300). The suspension was digested for 20 min in a 37 °C shaking water bath, tapering from 200 rpm to 100 rpm. The digestion reaction was stopped using ice cold MEM + LGA supplemented with 2 mg/mL gelatin (Sigma, G6650) and strained to remove undigested material. Clumps, which settle rapidly, were separated from the suspension of tubules during 2 rounds of pelleting and resuspension in ice cold MEM + LGA. The resulting tubules were then resuspended in ice-cold 37% Percoll (Cytiva, 17089101) solution with 5 mM glycine, 115 mM NaCl, 1.2 mM KH_2PO_4, 3.7 mM KCl, 1.2 mM $MgSO_4$, 1.2 mM $MgCl_2$, 1.25 mM $CaCl_2$, 25 mM $NaHCO_3$, and 20 mg/mL albumin (pH ~ 7.4 equilibrated with O_2/CO_2). The resuspension was then centrifuged at 3.7×10^4 g at 4 °C for 20 min, yielding 4 distinct layers consisting of glomeruli and debris, distal tubules, proximal tubules, and red blood cells. Proximal tubules were selectively aspirated and underwent several rounds of pelleting and resuspension in O_2/CO_2 equilibrated MEM + LGA supplemented with 2 mg/mL gelatin then culture medium to remove residual Percoll solution. Protein content was determined using the Bicinchoninic acid (BCA) assay (Thermo, 23227).

Quantification of purification efficiency

Both before and after Percoll gradient ultracentrifugation, samples of tubule suspensions were plated onto a poly-lysine coated slide, fixed, and then stained with 4',6-diamidino-2-phenylindole (1 µg/ml, DAPI) and fluorescein-conjugated lotus tetragonolobus lectin (1:100, LTL, Vector Labs, FL-1321) in situ. Slide images were acquired on a standard fluorescence microscope. Images were divided into 350 × 260 µm regions containing tubules, randomly sampled, randomly ordered, blinded, and manually assessed for the fraction of tubule length in each image positive for LTL. Data from at least 125 regions was averaged and reported for each experiment and condition.

Cell culture

For primary cultures, the final proximal tubule preparation was seeded on tissue culture treated polystyrene plates at 0.1 mg total protein/cm^2, unless otherwise stated. In some experiments, tubules were seeded on permeable culture inserts (Greiner Bio-one, 657640) at the same density. Culture medium was DMEM/F12 (Corning, 10092CM) with supplements as listed in Table 1. Medium was changed daily for the first 3 days after seeding, then every other day or as needed for a total of 14 days. Primary cells were never sub-cultured. Some experiments included variations in medium composition as indicated in the text. In some experiments, a TNFα antagonist (R-7050, 10 µM, Sigma, 654257), a NF-κB activation inhibitor (10 nM, Sigma, 481407) or DMSO vehicle were added directly to wells with each medium change. Cells were imaged using phase contrast and fluorescence microscopy at prespecified locations. Final confluency was estimated manually by a blinded observer in 5% increments for 4–8 regions per experiment and averaged. The immortalized mouse proximal cell line BUMPT was obtained from Dr. Wilfred Lieberthal[75]. These cells were cultured in DMEM supplemented with 10% fetal bovine serum (Sigma, F4135), penicillin (100 units/mL), and streptomycin (100 µg/mL) and sub-cultured near confluence every 3–5 days.

RNA isolation, purification, and analysis

Cells were rinsed with PBS. RNA was collected and purified using an RNeasy Mini Kit (Qiagen, 74104) including on-column DNase treatment. For RNA sequencing experiments, RNA was submitted to the Advanced Genomics Core at the University of Michigan for routine poly-A library preparation and subjected to 150 bp paired-end sequencing according to the manufacturer's protocol (Illumina NovaSeq) targeting 30 million reads per sample. Reads were aligned to the mouse genome (GRCm38 mm10) with the addition of custom sequences

Component	Final concentration	Supplier	Product number
Glucose	315 mg/dL	Corning	10092CM*
Bicarbonate	29 mM	Corning	10092CM*
HEPES	15 mM	Corning	10092CM*
Insulin-transferrin-selenium (ITS)	10 µg/mL, 5.5 µg/mL, 6.7 ng/mL	Corning	25-800-CR
EGF	10 ng/mL	R&D systems	236-EG-200
Hydrocortisone	36 ng/mL	Sigma	H6909-10ML
Ascorbate	50 µM	Sigma	A8960-5G
T3	10 pM	Sigma	T2752-100MG
Fetal bovine serum	0.5% v/v	Gibco	10437-028
Non-essential AA	1x	Gibco	15140-122
Penicillin	100 units/mL	Gibco	11140-050
Streptomycin	100 µg/mL	Gibco	11140-050

Table 1. Medium components. *As a part of the DMEM/F12 base, not all F12/DMEM components are reported.

for GFP transcripts. Differential expression was determined using DESeq2 (v1.38.2)[76]. Gene Set Enrichment Analysis (GSEA) was performed using the fgsea package in R[36] on differentially expressed genes determined by DESeq2 with $P_{adj} < 0.05$. In some cases, the normalized enrichment score was used as a measure of the degree of enrichment and plotted as a heatmap. Only analyses with significant enrichment ($P_{adj} < 0.05$) were shown. Heatmaps of expression were generated using transcripts per million (TPM) and were Z-score normalized across samples on a per-gene basis. Differentially expressed genes were submitted to ChEA3[39] using the web interface. The output was downloaded and provided in Supplementary Data S3. All raw count and TPM data are available in Supplementary Datas S1 and Data S4.

Quantitative real-time RT-PCR was also performed on RNA samples obtained from experiments independent from those used for RNA-seq. Reverse transcription was performed using the HighCapacity cDNA Reverse Transcription Kit (Thermo, 4368814) per manufacturer instructions using random primers. PCR was performed using a 7500 Real Time PCR System (Applied Biosystems, Thermo) with SYBR Green master mix (Bio-Rad, 1725121), according to manufacturer instructions with primers listed in Supplementary Table S1. Data was normalized to β-actin then to fresh tubules (delta-delta Ct method).

Western blot

Cells were rinsed with PBS. Samples were then incubated with 20 μL/cm^2 radioimmunoprecipitation assay (RIPA) buffer with protease inhibitors (Santa Cruz Biotechnology, sc-24948) and 5 mM sodium fluoride on ice for 20 min. Insoluble material was collected by centrifugation at 17,000×*g* for 10 min at 4 °C. Protein concentration in the supernatant was determined using the bicinchoninic acid (BCA) assay. Samples were then mixed with concentrated sodium dodecyl sulfate (SDS) loading buffer and heated at 95 °C for 5 min prior to use. 10 μg of protein was loaded in 4–15% SDS-polyacrylamide gel electrophoresis (PAGE) gradient gels (Bio-Rad) followed by electrophoresis for 1 to 1.5 h. Protein was transferred to a polyvinylidene fluoride (PVDF) membrane (Millipore Sigma, IPFL00010). Membranes were blocked with dehydrated milk and incubated with primary antibodies against HNF4A (1:1000, Abcam, AB201460). After rinsing, the membrane was incubated with an HRP-labeled secondary antibody. Signal was detected using enhanced chemiluminescence (ECL) reagent (Thermo, 32209) and autoradiography film. Membranes were then stripped and re-probed for β-actin (1:10,000, Cell Signaling Technology, 4970) as a loading control.

Immunostaining

Cultured cells were fixed in situ with 4% formaldehyde in PBS for 10 min at room temperature, rinsed, and stored in PBS at 4 °C. Samples were permeabilized with 0.5% Triton-X 100 in PBS, blocked with 20 mg/mL bovine serum albumin, and incubated for 4 h at room temperature with anti-ZO-1 (1:800, Thermo, 33-9100) or anti-Na-K ATPase (1:200, Santa Cruz, sc-48345), rinsed, incubated with isotype-specific secondary antibodies, rinsed, and mounted under glass coverslips with ProLong Diamond antifade mounting medium (Thermo, P36971) for long-term storage. Samples were imaged using a standard fluorescence microscope. Focal areas with basolateral Na-K ATPase staining were imaged with a confocal microscope.

Some paraffin embedded kidney sections were also stained and imaged as described previously[38,77]. Briefly, explanted kidneys were fixed in 4% formaldehyde/PBS overnight, embedded in paraffin, and sectioned at ~ 5 μm thickness. Mounted sections were deparaffinized and rehydrated using a graded series of xylene-ethanol-water solutions. Slides were treated with either citrate- or tris-based antigen unmasking solution (Vector Laboratories, depending on primary antibodies used, H-3300 or H-3301) in a pressure cooker for 10 min. Samples were then permeabilized with 0.5% Triton-X 100 in PBS, blocked with 20 mg/mL bovine serum albumin, and incubated overnight with primary antibodies (anti-villin, 1:400, Santa Cruz, sc-58897; anti-OAT-1, 1:400, Proteintech, 26574-1-AP, anti-GFP, 1:400, Santa Cruz, sc-9996, for nT/nG; anti-GFP, Thermo, A10262, for mT/mG) in 0.1% Tween-20 in PBS (PBS-T). Sections were then extensively rinsed with PBS-T and incubated with species-specific fluorophore-conjugated secondary antibodies in PBS-T for 2 h at room temperature, rinsed with PBS-T, then PBS, then water, and quickly dried. Hydrophobic pen (which interferes with automated slide scanning) was removed by immersing the slides in xylene for 60 s. Xylene was then quickly evaporated and the slides rehydrated in PBS. Slides were then treated with the TrueVIEW autofluorescence quenching kit (Vector Labs, SP-8500). Samples were counterstained with 1 μg/mL DAPI. Samples were mounted with Vectashield mounting medium (Vector Labs, SP-8500), allowed to cure overnight at room temperature, and stored at 4 °C protected from light until scanning.

Quantification of in vivo labeling fraction

Stained samples were analyzed as previously described[38,77]. Briefly, stained sections were scanned at a resolution of 0.5 μm per pixel using a Vectra Polaris whole slide scanner (Akoya). Proximal tubule segments were assigned based on histologic location. The border between S2 and S3 proximal tubule was defined using villin, which labels the entire proximal tubule, and OAT-1, which labels predominantly S2 proximal tubule. Tubules on the medullary side of this border were assumed to be predominantly S3, tubules on the cortical side of this border were assumed to be predominantly S1 and S2. U-Net[78] deep learning models were trained to identify all DAPI-stained nuclei, all villin + proximal tubules, and GFP-labeled nuclei. The U-Net model for GFP nuclei was trained to ignore bleed through of OAT-1 signal into the GFP channel, which was present in some samples. Each nucleus (51,725−128,079 nuclei analyzed per sample) was classified by villin status, GFP status, and segment (S1-S2 vs. S3). Data were reported for each segment as fraction of GFP + villin + per total villin + nuclei, representing the fraction of labeled proximal tubules in each segment.

Proximal tubule fate tracing in culture

Tubules derived from proximal tubule reporter mice (mT/mG or nT/nG) were prepared and cultured as with wild type mice. Fluorescence images were obtained at pre-specified locations during culture (0–14 days) to follow the evolution of specific areas. For experiments using mT/mG mice, images were analyzed by thresholding images in ImageJ[79]. The area of red (tdTomato) and green (GFP) were measured and any overlapping areas were assigned as GFP. Mice contained two alleles of the GFP reporter and can occasionally express both tdTomato and GFP, but any GFP expression indicates Cre activity and proximal tubule origin. For experiments using nT/nG mice, images were analyzed using U-Net segmentation[78] followed by the Analyze Particles function in ImageJ to identify nuclei. Costained nuclei were considered GFP + only. Until cells established colonies (~2 days), the individual nuclei of 3-dimensional tubules could not be distinguished consistently. Analysis of nT/nG animals was only performed for 2 days and later.

HNF4A overexpression

A retrovirus vector was generated using an HNF4A overexpression (HNF4A-OE) vector[44] (Addgene plasmid #33006). BUMPT cells were transduced overnight, rinsed, and subcultured as single cell clones. Transduced clones were selected by GFP expression via an internal ribosome entry site (IRES) following the 3' end of the HNF4A transcript. GFP negative control clones were also selected. 3 independent HNF4A-OE clones and 3 controls were cultured to confluence and subjected to RNA-seq.

Statistics

Data are presented as mean ± standard deviation unless otherwise specified. Each data point represents an independent tubule isolation from 2 to 3 mice. Statistical analysis was performed using the test indicated in R (version 4.3.1, transcriptomic analyses) or GraphPad Prism (version 10.2.1, all other analyses). Parametric tests were used for continuous or near continuous normally distributed data. Non-parametric tests were used for other data types.

Data availability

The datasets used in the current study have been deposited in the Gene Expression Omnibus, accession GSE273058.

Received: 25 March 2024; Accepted: 22 September 2024
Published online: 02 October 2024

References

1. Humes, H. D. Tissue engineering of a bioartificial kidney: a universal donor organ. *Transpl. Proc.* **28**, 2032–2035 (1996).
2. Oxburgh, L. et al. Re)building a kidney. *J. Am. Soc. Nephrol.* **28**, 1370–1378. https://doi.org/10.1681/ASN.2016101077 (2017).
3. Kim, E. J. et al. Feasibility of an implantable bioreactor for renal cell therapy using silicon nanopore membranes. *Nat. Commun.* **14**, 4890. https://doi.org/10.1038/s41467-023-39888-2 (2023).
4. Ferrell, N., Ricci, K. B., Groszek, J., Marmerstein, J. T. & Fissell, W. H. Albumin handling by renal tubular epithelial cells in a microfluidic bioreactor. *Biotechnol. Bioeng.* **109**, 797–803. https://doi.org/10.1002/bit.24339 (2012).
5. Kelly, E. J. et al. Innovations in preclinical biology: ex vivo engineering of a human kidney tissue microperfusion system. *Stem Cell Res. Ther.* **4**. https://doi.org/10.1186/scrt378 (2013).
6. Weber, E. J. et al. Development of a microphysiological model of human kidney proximal tubule function. *Kidney Int.* **90**, 627–637. https://doi.org/10.1016/j.kint.2016.06.011 (2016).
7. Rayner, S. G. et al. Reconstructing the human renal vascular–tubular unit in Vitro. *Adv. Healthc. Mater.* **1801120**. https://doi.org/10.1002/adhm.201801120 (2018).
8. Aleo, M. D. & Schnellmann, R. G. Regulation of glycolytic metabolism during long-term primary culture of renal proximal tubule cells. *Am. J. Physiol.* **262**, 85. https://doi.org/10.1152/ajprenal.1992.262.1.F77 (1992).
9. Nowak, G. & Schnellmann, R. G. Improved culture conditions stimulate gluconeogenesis in primary cultures of renal proximal tubule cells. *Am. J. Physiol.* **268**, 61. https://doi.org/10.1152/ajpcell.1995.268.4.C1053 (1995).
10. Tang, M. J., Suresh, K. R. & Tannen, R. L. Carbohydrate metabolism by primary cultures of rabbit proximal tubules. *Am. J. Physiol.* **256**, 9. https://doi.org/10.1152/ajpcell.1989.256.3.C532 (1989).
11. Tang, M. J. & Tannen, R. L. Metabolic substrates alter attachment and differentiated functions of proximal tubule cell culture. *J. Am. Soc. Nephrology: JASN.* **4**, 1908–1911 (1994).
12. Love, H. D. et al. Substrate elasticity governs differentiation of renal tubule cells in prolonged culture. *Tissue Eng. Part A*. https://doi.org/10.1089/ten.tea.2018.0182 (2018).
13. Beamish, J. A., Chen, E. & Putnam, A. J. Engineered extracellular matrices with controlled mechanics modulate renal proximal tubular cell epithelialization. *PLOS ONE* **12**, 1. https://doi.org/10.1371/journal.pone.0181085 (2017).
14. Westover, A. J., Buffington, D. A. & Humes, H. D. Enhanced propagation of adult human renal epithelial progenitor cells to improve cell sourcing for tissue-engineered therapeutic devices for renal diseases. *J. Tissue Eng. Regen. Med.* **6**, 589–597. https://doi.org/10.1002/term.471 (2012).
15. Hoppensack, A. et al. A human in Vitro Model that mimics the renal proximal tubule. *Tissue Eng. Part. C: Methods*. **20**, 599–609. https://doi.org/10.1089/ten.tec.2013.0446 (2014).
16. Vanslambrouck, J. M., Tan, K. S., Mah, S. & Little, M. H. Generation of proximal tubule-enhanced kidney organoids from human pluripotent stem cells. *Nat. Protoc.* **18**, 3229–3252. https://doi.org/10.1038/s41596-023-00880-1 (2023).
17. Morizane, R. & Bonventre, J. V. Generation of nephron progenitor cells and kidney organoids from human pluripotent stem cells. *Nat. Protoc.* **12**, 195–207. https://doi.org/10.1038/nprot.2016.170 (2016).
18. Khundmiri, S. J., Chen, L., Lederer, E. D., Yang, C. R. & Knepper, M. A. Transcriptomes of major proximal tubule cell culture models. *J. Am. Soc. Nephrol.* **32**, 86–97. https://doi.org/10.1681/asn.2020010009 (2020).
19. Ferrell, N. et al. Application of physiological shear stress to renal tubular epithelial cells. *Methods Cell. Biol.* **153**, 43–67. https://doi.org/10.1016/bs.mcb.2019.04.010 (2019). PMID – 31395384.
20. Ferrell, N., Cheng, J., Miao, S., Roy, S. & Fissell, W. H. Orbital Shear Stress Regulates Differentiation and Barrier Function of Primary Renal Tubular Epithelial Cells. *ASAIO J. Online First* **1**, 1. https://doi.org/10.1097/MAT.0000000000000723 (2017).
21. Griner, R. D., Aleo, M. D. & Schnellmann, R. G. The role of short chain fatty acid substrates in aerobic and glycolytic metabolism in primary cultures of renal proximal tubule cells. *In Vitro Cell. Dev. Biol. Anim.* **29A**, 649–655 (1993).

22. Chung, S. D., Alavi, N., Livingston, D., Hiller, S. & Taub, M. Characterization of primary rabbit kidney cultures that express proximal tubule functions in a hormonally defined medium. *J. Cell Biol.* **95**, 118–126. https://doi.org/10.1083/jcb.95.1.118 (1982).
23. Borza, C. M. et al. DDR1 contributes to kidney inflammation and fibrosis by promoting the phosphorylation of BCR and STAT3. *JCI Insight*. https://doi.org/10.1172/jci.insight.150887 (2021).
24. Park, J. S., Pasupulati, R., Feldkamp, T., Roeser, N. F. & Weinberg, J. M. Cyclophilin D and the mitochondrial permeability transition in kidney proximal tubules after hypoxic and ischemic injury. *Am. J. Physiol. Renal Physiol.* **301**, F134–F150. https://doi.org/10.1152/ajprenal.00033.2011 (2011).
25. Bienholz, A. et al. Substrate modulation of fatty Acid effects on energization and respiration of kidney proximal tubules during Hypoxia/Reoxygenation. *PLoS ONE*. **9**, e94584. https://doi.org/10.1371/journal.pone.0094584 (2014).
26. Nowak, G. & Schnellmann, R. G. L-ascorbic acid regulates growth and metabolism of renal cells: improvements in cell culture. *Am. J. Physiol.* **271**, 80. https://doi.org/10.1152/ajpcell.1996.271.6.C2072 (1996).
27. Linkermann, A. et al. Synchronized renal tubular cell death involves ferroptosis. *Proc. Natl. Acad. Sci.* **111**, 16836–16841. https://doi.org/10.1073/pnas.1415518111 (2014).
28. Lee, J. W., Chou, C. L. & Knepper, M. A. Deep sequencing in microdissected renal tubules identifies nephron segment-specific transcriptomes. *J. Am. Soc. Nephrol.* **26**, 2669–2677. https://doi.org/10.1681/ASN.2014111067 (2015).
29. Chen, L., Chou, C. L. & Knepper, M. A. A Comprehensive Map of mRNAs and their isoforms across all 14 renal tubule segments of mouse. *J. Am. Soc. Nephrol.* **32**, 897–912. https://doi.org/10.1681/asn.2020101406 (2021).
30. Kirita, Y., Wu, H., Uchimura, K., Wilson, P. C. & Humphreys, B. D. Cell profiling of mouse acute kidney injury reveals conserved cellular responses to injury. *Proc. Natl. Acad. Sci.* **117**, 15874–15883. https://doi.org/10.1073/pnas.2005477117 (2020).
31. Liberzon, A. et al. The molecular signatures database hallmark gene set collection. *Cell. Syst.* **1**, 417–425. https://doi.org/10.1016/j.cels.2015.12.004 (2015).
32. Mariani, L. H. et al. Precision nephrology identified tumor necrosis factor activation variability in minimal change disease and focal segmental glomerulosclerosis. *Kidney Int.* **103**, 565–579. https://doi.org/10.1016/j.kint.2022.10.023 (2023).
33. Ide, S. et al. Ferroptotic stress promotes the accumulation of pro-inflammatory proximal tubular cells in maladaptive renal repair. *eLife* **10**, e68603. https://doi.org/10.7554/elife.68603 (2021).
34. Gerhardt, L. M. S. et al. Lineage tracing and single-nucleus Multiomics Reveal Novel features of adaptive and maladaptive repair after Acute kidney Injury. *J. Am. Soc. Nephrol.* **34**, 554–571. https://doi.org/10.1681/asn.0000000000000057 (2023).
35. Gerhardt, L. M. S., Liu, J., Koppitch, K., Cippà, P. E. & McMahon, A. P. Single-nuclear transcriptomics reveals diversity of proximal tubule cell states in a dynamic response to acute kidney injury. *Proc. Natl. Acad. Sci. U.S.A.* **118**, e2026684118. https://doi.org/10.1073/pnas.2026684118 (2021).
36. Korotkevich, G. et al. Fast gene set enrichment analysis. *bioRxiv* **1**, 060012. https://doi.org/10.1101/060012 (2021).
37. Subramanian, A. et al. Gene set enrichment analysis: A knowledge-based approach for interpreting genome-wide expression profiles. *Proc. Natl. Acad. Sci.* **102**, 15545–15550. https://doi.org/10.1073/pnas.0506580102 (2005).
38. Beamish, J. A. et al. Pax protein depletion in proximal tubules triggers conserved mechanisms of resistance to acute ischemic kidney injury preventing transition to chronic kidney disease. *Kidney Int.* **105**, 312–327. https://doi.org/10.1016/j.kint.2023.10.022 (2024).
39. Keenan, A. B. et al. ChEA3: transcription factor enrichment analysis by orthogonal omics integration. *Nucleic Acids Res.* **47**, W212–W224. https://doi.org/10.1093/nar/gkz446 (2019). PMID – 31114921.
40. Xu, S. et al. Nuclear farnesoid X receptor attenuates acute kidney injury through fatty acid oxidation. *Kidney Int.* **101**, 987–1002. https://doi.org/10.1016/j.kint.2022.01.029 (2022). PMID – 35227690.
41. Yoshimura, Y., Muto, Y., Omachi, K., Miner, J. H. & Humphreys, B. D. Elucidating the proximal tubule HNF4A gene regulatory network in human kidney organoids. *J. Am. Soc. Nephrol.*https://doi.org/10.1681/asn.0000000000000197 (2023).
42. Marable, S. S., Chung, E. & Park, J. S. Hnf4a is required for the development of Cdh6-Expressing progenitors into proximal tubules in the mouse kidney. *J. Am. Soc. Nephrol.* **31**, 2543–2558. https://doi.org/10.1681/asn.2020020184 (2020).
43. Kaminski, M. M. et al. Direct reprogramming of fibroblasts into renal tubular epithelial cells by defined transcription factors. *Nat. Cell Biol.* **18**, 1269–1280. https://doi.org/10.1038/ncb3437 (2016).
44. Sekiya, S. & Suzuki, A. Direct conversion of mouse fibroblasts to hepatocyte-like cells by defined factors. *Nature*. **475**, 390–393. https://doi.org/10.1038/nature10263 (2011).
45. Kim, J. Y. et al. SOX9 promotes stress-responsive transcription of VGF nerve growth factor inducible gene in renal tubular epithelial cells. *J. Biol. Chem.* **295**, 16328–16341. https://doi.org/10.1074/jbc.ra120.015110 (2020).
46. Kim, J. Y. et al. A kinome-wide screen identifies a CDKL5-SOX9 regulatory axis in epithelial cell death and kidney injury. *Nature Commun.* **11**. https://doi.org/10.1038/s41467-020-15638-6 (2020).
47. Kayampilly, P., Roeser, N., Rajendiran, T. M., Pennathur, S. & Afshinnia, F. Acetyl Co-A Carboxylase inhibition halts hyperglycemia induced upregulation of de novo lipogenesis in podocytes and proximal tubular cells. *Metabolites* **12**, 940. https://doi.org/10.3390/metabo12100940 (2022).
48. Wang, Y. & Taub, M. Insulin and other regulatory factors modulate the growth and the phosphoenolpyruvate carboxykinase (PEPCK) activity of primary rabbit kidney proximal tubule cells in serum free medium. *J. Cell. Physiol.* **147**, 374–382. https://doi.org/10.1002/jcp.1041470224 (1991).
49. Nowak, G. & Schnellmann, R. G. Integrative effects of EGF on metabolism and proliferation in renal proximal tubular cells. *Am. J. Physiol.* **269**, 25. https://doi.org/10.1152/ajpcell.1995.269.5.C1317 (1995).
50. Humes, H. D. & Cieslinski, D. A. Interaction between growth factors and retinoic acid in the induction of kidney tubulogenesis in tissue culture. *Exp. Cell Res.* **201**, 8–15. https://doi.org/10.1016/0014-4827(92)90342-6 (1992).
51. Elliget, K. A. & Trump, B. F. Primary cultures of normal rat kidney proximal tubule epithelial cells for studies of renal cell injury. *Vitro Cell. Dev. Biol. Anim.* **27**, 739–748. https://doi.org/10.1007/bf02633220 (1991).
52. Johnson, D. W. et al. Transport characteristics of human proximal tubule cells in primary culture. *Nephrology*. **3**, 183–194. https://doi.org/10.1111/j.1440-1797.1997.tb00213.x (1997).
53. Harris, R. C. & Daniel, T. O. Epidermal growth factor binding, stimulation of phosphorylation, and inhibition of gluconeogenesis in rat proximal tubule. *J. Cell. Physiol.* **139**, 383–391. https://doi.org/10.1002/jcp.1041390222 (1989).
54. Lake, B. B. et al. An atlas of healthy and injured cell states and niches in the human kidney. *Nature*. **619**, 585–594. https://doi.org/10.1038/s41586-023-05769-3 (2023).
55. Ruegg, C. E. & Mandel, L. J. Bulk isolation of renal PCT and PST. I. glucose-dependent metabolic differences. *Am. J. Physiol. Renal Physiol.* **259**, F164–F175. https://doi.org/10.1152/ajprenal.1990.259.1.f164 (1990).
56. Rankin, E. B., Tomaszewski, J. E. & Haase, V. H. Renal Cyst Development in mice with conditional inactivation of the Von Hippel-Lindau Tumor suppressor. *Cancer Res.* **66**, 2576–2583. https://doi.org/10.1158/0008-5472.can-05-3241 (2006).
57. Chang-Panesso, M. et al. FOXM1 drives proximal tubule proliferation during repair from acute ischemic kidney injury. *J. Clin. Invest.*https://doi.org/10.1172/JCI125519 (2019).
58. Piret, S. E. et al. Loss of proximal tubular transcription factor Krüppel-like factor 15 exacerbates kidney injury through loss of fatty acid oxidation. *Kidney Int.* **100**, 1250–1267. https://doi.org/10.1016/j.kint.2021.08.031 (2021).
59. Dickman, K. G. & Mandel, L. J. Glycolytic and oxidative metabolism in primary renal proximal tubule cultures. *Am. J. Physiology-Cell Physiol.* **257**, C333–C340. https://doi.org/10.1152/ajpcell.1989.257.2.c333 (1989).
60. McLimans, W. F., Blumenson, L. E. & Tunnah, K. V. Cell Culture systems. 11. Theory. *Biotechnol. Bioeng.* **10**, 741–763. https://doi.org/10.1002/bit.260100604 (1968).

61. Werrlein, R. J. & Glinos, A. D. Oxygen microenvironment and respiratory oscillations in cultured mammalian cells. *Nature*. **251**, 317–319 (1974).
62. Stevens, K. M. Oxygen requirements for liver cells in vitro. *Nature*. **206**, 199–199. https://doi.org/10.1038/206199a0 (1965).
63. Venkatachalam, M. A., Weinberg, J. M., Kriz, W. & Bidani, A. K. Failed tubule recovery, AKI-CKD transition, and kidney disease progression. *J. Am. Soc. Nephrol.* **26**, 1765–1776. https://doi.org/10.1681/ASN.2015010006 (2015).
64. Ferenbach, D. A. & Bonventre, J. V. Mechanisms of maladaptive repair after AKI leading to accelerated kidney ageing and CKD. *Nat. Rev. Nephrol.* **11**, 264–276. https://doi.org/10.1038/nrneph.2015.3 (2015).
65. Sato, Y. et al. Hypoxia reduces HNF4α/MODY1 protein expression in pancreatic β-cells by activating AMP-activated protein kinase. *J. Biol. Chem.* **292**, 8716–8728. https://doi.org/10.1074/jbc.m116.767574 (2017). PMID – 28364040.
66. Gilglioni, E. H. et al. Improved oxygenation dramatically alters metabolism and gene expression in cultured primary mouse hepatocytes. *Hepatol. Commun.* **2**, 299–312. https://doi.org/10.1002/hep4.1140 (2018). PMID – 29507904.
67. Ferrell, N. et al. A microfluidic bioreactor with integrated transepithelial electrical resistance (TEER) measurement electrodes for evaluation of renal epithelial cells. *Biotechnol. Bioeng.* **107**, 707–716. https://doi.org/10.1002/bit.22835 (2010).
68. Chen, W. C., Lin, H. H. & Tang, M. J. Regulation of proximal tubular cell differentiation and proliferation in primary culture by matrix stiffness and ECM components. *Am. J. Physiol. - Ren. Physiol.* **307**https://doi.org/10.1152/ajprenal.00684.2013 (2014).
69. Love, H. et al. Metformin and inhibition of transforming growth factor-Beta stimulate in Vitro Transport in primary renal tubule cells. *Tissue Eng. Part A*. **26**, 1091–1098. https://doi.org/10.1089/ten.tea.2019.0294 (2020).
70. Hunter, K. et al. Inhibition of transforming growth Factor-β improves primary renal tubule cell differentiation in long-term culture. *Tissue Eng. Part A*. **29**, 102–111. https://doi.org/10.1089/ten.tea.2022.0147 (2023). PMID – 36274231.
71. Lan, R. et al. PTEN loss defines a TGF-β-induced tubule phenotype of failed differentiation and JNK signaling during renal fibrosis. *Am. J. Physiol. Ren. Physiol.* **302**, F1210–1223. https://doi.org/10.1152/ajprenal.00660.2011 (2012).
72. Morizane, R. et al. Nephron organoids derived from human pluripotent stem cells model kidney development and injury. *Nat. Biotechnol.* **33**, 1193–1200. https://doi.org/10.1038/nbt.3392 (2015).
73. Aceves, J. O. et al. 3D proximal tubule-on-chip model derived from kidney organoids with improved drug uptake. *Sci. Rep.* **12**, 14997. https://doi.org/10.1038/s41598-022-19293-3 (2022).
74. Muzumdar, M. D., Tasic, B., Miyamichi, K., Li, L. & Luo, L. A global double-fluorescent Cre reporter mouse. *Genesis* **45**, 593–605. https://doi.org/10.1002/dvg.20335 (2007).
75. Sinha, D., Wang, Z., Price, V. R., Schwartz, J. H. & Lieberthal, W. Chemical anoxia of tubular cells induces activation of c-Src and its translocation to the zonula adherens. *Am. J. Physiol. Renal Physiol.* **284**, F488–F497. https://doi.org/10.1152/ajprenal.00172.2002 (2003).
76. Love, M. I., Huber, W. & Anders, S. Moderated estimation of Fold change and dispersion for RNA-seq data with DESeq2. *Genome Biol.* **15**, 550. https://doi.org/10.1186/s13059-014-0550-8 (2014).
77. McElliott, M. C. et al. High-throughput image analysis with deep learning captures heterogeneity and spatial relationships after kidney injury. *Sci. Rep.* **13**, 6361. https://doi.org/10.1038/s41598-023-33433-3 (2023).
78. Falk, T. et al. U-Net: deep learning for cell counting, detection, and morphometry. *Nat. Methods*. **16**, 67–70. https://doi.org/10.1038/s41592-018-0261-2 (2019). PMID – 30559429.
79. Schneider, C. A., Rasband, W. S. & Eliceiri, K. W. NIH Image to ImageJ: 25 years of image analysis. *Nat. Methods*. **9**. https://doi.org/10.1038/nmeth.2089 (2012).

Acknowledgements

We would like to thank Gregory Dressler, Sanjeevkumar Patel, and Joel Weinberg for their helpful suggestions in the development of this project. Support for this work was provided by the University of Michigan O'Brien Kidney Center (DK-P30-081943 to J.A.B.),NIH K08 DK125776 (to J.A.B.), and an American Society of Nephrology KidneyCure Carl W. Gottschalk Research Scholar Grant (to J.A.B.).

Author contributions

J.A.B. designed the research. A.C.T., J.T.F-S., M.C.M., M.C., and J.A.B. performed experiments. A.C.T., M.C.M., J.T.F-S., and J.A.B. analyzed and interpreted results. A.C.T. and J.A.B. wrote the manuscript with contributions from all authors.

Declarations

Competing interests

The authors declare no competing interests.

Additional information

Supplementary Information The online version contains supplementary material available at https://doi.org/10.1038/s41598-024-73861-3.

Correspondence and requests for materials should be addressed to J.A.B.